

Proton-proton elastic scattering at 6.0 GeV/c with three spins measured*

L. G. Ratner

Accelerator Research Facilities Division, Argonne National Laboratory, Argonne, Illinois 60439

M. Borghini

CERN, Geneva 23, Switzerland

W. de Boer,[†] R. C. Fernow, A. D. Krisch,[‡] H. E. Miettinen,[§] T. A. Mulera, J. B. Roberts,^{||}
and K. M. Terwilliger

Randall Laboratory of Physics, The University of Michigan, Ann Arbor, Michigan 48109

J. R. O'Fallon

Department of Physics, St. Louis University, St. Louis, Missouri 63103

(Received 22 October 1976)

The differential elastic p - p scattering cross section was measured at 6 GeV/c at the Argonne Zero Gradient Synchrotron in the range $P_{\perp}^2 = 0.6-1.0$ (GeV/c)² using a 65%-polarized target and a 75%-polarized extracted beam of intensity 3×10^9 protons/pulse. We simultaneously measured the polarization of the recoil proton with a well-calibrated carbon-target polarimeter. All three polarizations were measured perpendicular to the horizontal scattering plane. Our results indicate that P and T invariance are both obeyed to good precision even at large P_{\perp}^2 . Parity invariance implies that the eight single-flip transversity cross sections are zero, so our data give the relative magnitudes of the eight remaining pure spin cross sections where all spins are measured. We find that the double-flip transversity cross sections are nonzero.

It is becoming more and more apparent that spin effects play an important role in high-energy strong interactions. The Zero Gradient Synchrotron (ZGS) polarized beam allows precise studies of these spin effects, especially when used with a polarized target. During the past few years our group¹ and the ANL-Northwestern group² have used the ZGS to study the spin dependence of proton-proton elastic scattering. We previously reported^{1,3} significant differences between the various 6-GeV/c pure two-spin transversity cross sections (with both initial spins measured). We also measured³ the polarization of the recoil proton at $P_{\perp}^2 = 0.5$ (GeV/c)² and found some evidence for a nonzero double-spin-flip cross section. The present experiment extends these 6-GeV/c three-spin measurements to $P_{\perp}^2 = 0.6, 0.8,$ and 1.0 (GeV/c)². A number of changes improved the experiment: The direction of the beam polarization was reversed on alternate pulses; the accelerated intensity was increased to 3×10^9 protons/pulse with a 2.5-sec repetition rate; the recoil polarimeter was redesigned to tighten its angular resolution and was directly calibrated using the ZGS polarized beam.

The experimental apparatus is similar to that used in our earlier measurements^{1,3} and will be described in detail in a coming publication.⁴ The beam polarization, P_B , was measured using a high-energy polarimeter consisting of a liquid

hydrogen target and two double-arm spectrometers, each containing magnets and scintillation counters. The polarimeter measured the left-right asymmetry in pp elastic scattering at 6.0 GeV/c and $P_{\perp}^2 = 0.5$ (GeV/c)². The beam polarization is given by

$$P_B = \frac{1}{A} \left(\frac{L - R}{L + R} \right), \quad (1)$$

where L is the number of coincidences in the left arm, R is the number in the right arm, and $A = 0.100 \pm 0.006$ is the asymmetry parameter for p - p elastic scattering. The average beam polarization was $P_B = (75 \pm 5)\%$.

We scattered the polarized beam from the Michigan-Argonne PPT V polarized proton target.^{1,3,4} The target consists of frozen beads of propanediol, $C_3H_8O_2$, doped with Cr^V paramagnetic complexes. The beads are 1-2 mm in diameter and are contained in a 4-cm-long by 3-cm-diameter target cavity. The target is maintained at 0.5 °K in a magnetic field of 25 kG which polarized the Cr^V electrons. The proton polarization, P_T , is produced by 70-GHz microwaves using the dynamic polarization technique and measured using a 107-MHz NMR system with signal averaging. The target protons' polarization has been as high as 85%, but radiation damage to the target beads reduced the average P_T to $(65 \pm 4)\%$. Two NMR coils of different diameters averaged

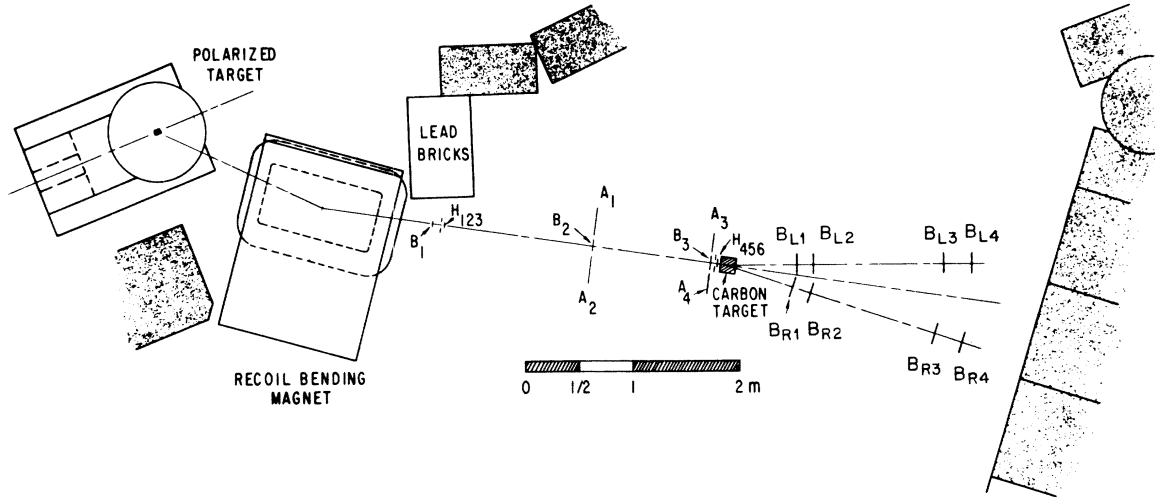


FIG. 1. Layout of the recoil (B) arm and the B polarimeter. The recoil proton is momentum-analyzed by the recoil magnet and then detected by the $B_1 B_2 B_3$ counters. The H_{123} and H_{456} hodoscopes monitor its angle and position prior to its scattering from the carbon target, while the B_L and B_R telescopes detect the p - C scattering to the left and the right. The A counters reduce background.

out the spatial dependence of the polarization due to beam-induced radiation damage. The direction of the target polarization was reversed approximately every 12 hours.

Elastic scattering events from the polarized target were detected in another double-arm spectrometer^{1,3,4}; the recoil arm of this is shown in Fig. 1. Elastic events were determined by coincidences ($FB\bar{A}$) between the forward (F) and the recoil or backward (B) protons in which the anticounters A did not fire. The nominally defining forward counter F_3 , which was about 15 cm \times 13 cm (horizontal \times vertical) and about 18.4 m from the PPT, subtended a solid angle of $\Delta\Omega_{lab} \sim 57 \mu\text{sr}$, and had a momentum bite $\Delta P/P \sim 7\%$. The $FB\bar{A}$ accidentals, which were about $\frac{1}{4}\%$ of $FB\bar{A}$, were continuously monitored and subtracted. We measured our inelastic background by substituting Teflon beads for the propanediol and by running event rate curves while varying the recoil magnet current. This background was $(3.9 \pm 0.2)\%$ and was subtracted from the measured $FB\bar{A}$ rates.

The polarization of the recoil proton (P_R) was measured with the B polarimeter shown in Fig. 1. Approximately 0.8% of the recoil protons re-scatter from a 13-cm-long carbon target into four-fold scintillation-counter telescopes subtending the range $\theta_{lab} = 7^\circ - 11^\circ$. The defining counters B_{L4} and B_{R4} were about 17 cm \times 40 cm (h \times v) and about 2.3 m from the carbon target. We measured the asymmetry A_m in p -carbon scat-

tering,

$$A_m = \frac{B_L - B_R}{B_L + B_R}, \quad (2)$$

where $B_L = FB\bar{A} \cdot B_{L1} B_{L2} B_{L3} B_{L4}$, $B_R = FB\bar{A} \cdot B_{R1} B_{R2} B_{R3} B_{R4}$, and $FB\bar{A}$ is the elastic-event trigger. We then obtained the recoil proton's polarization P_R from the equation

$$P_R = \frac{A_m - D}{A_C - A_m E}, \quad (3)$$

where A_C is essentially the p - C analyzing power or asymmetry parameter for the polarimeter. D and E reflect biases of the polarimeter due to counter inefficiency, surveying or construction errors, and the angular and positional variation of the recoil protons heading into the carbon target. D and E were as large as 10% and had to be known along with A_C for all possible recoil-proton angles and positions.

We measured the incident angle and position using two overlapping five-channel hodoscopes ($H_1 H_{12} H_2 H_{23} H_3$ and $H_4 H_{45} H_5 H_{56} H_6$) placed just upstream of the carbon target. Each event that triggered an $FB\bar{A}$ coincidence was assigned to one channel of a 5×5 matrix. This information was recorded in a CAMAC discriminator coincidence register (DCR) coupled to a PDP11/10, which also recorded if B_L and B_R had fired.

The Teflon background runs gave a $B_L + B_R$ rate of $(3.9 \pm 0.7)\%$ of the normal rate at both $P_{\perp}^2 = 0.6$ and $1.0 (\text{GeV}/c)^2$, and within statistics B_L and B_R

TABLE I. Summary of Wolfenstein parameters at 6.0 GeV/c. The errors shown are point to point only. In addition, there are normalization errors of ± 0.005 on A and C_{nn} and $\pm 5\%$ of the value of D_{nn} and K_{nn} .

| P_{\perp}^2 [(GeV/c) 2] | A | C_{nn} | D_{nn} | K_{nn} |
|-------------------------------|-------------------|-------------------|-----------------|-----------------|
| 0.6 | 0.091 ± 0.003 | 0.107 ± 0.004 | 0.85 ± 0.03 | 0.13 ± 0.03 |
| 0.8 | 0.092 ± 0.003 | 0.080 ± 0.004 | 0.83 ± 0.04 | 0.05 ± 0.04 |
| 1.0 | 0.144 ± 0.003 | 0.057 ± 0.004 | 0.76 ± 0.05 | 0.04 ± 0.05 |

were equal. We therefore made a 3.9% subtraction from both B_L and B_R at all three P_{\perp}^2 values. Two types of accidentals were monitored. The accidental rate between $FB\bar{A} \cdot B_{L12}$ and B_{L34} was typically $(2.7 \pm 0.2)\%$ of the B_L rate. The accidentals between $FB\bar{A}$ and B_{L1234} were typically $(0.3 \pm 0.1)\%$ of the B_L rate. Both types were monitored continuously for both B_L and B_R and were subtracted.

We calibrated the hodoscope-polarimeter system by physically moving it into the main ZGS polarized beam and taking calibration runs with the polarized beam accelerated to the appropriate recoil momentum for each P_{\perp}^2 value: 870 MeV/c for $P_{\perp}^2 = 0.6$, 1050 MeV/c for $P_{\perp}^2 = 0.8$, and 1220 MeV/c for $P_{\perp}^2 = 1.0$ (GeV/c) 2 . The calibration runs gave values of A_C , D , and E for each of the 25 hodoscope channels with about 1% precision. These values were used in Eq. (3) to obtain P_R . The hodoscope-polarimeter had a large average analyzing power: A_C was 59.2% at $P_{\perp}^2 = 0.6$, 44.6% at $P_{\perp}^2 = 0.8$, and 31.6% at $P_{\perp}^2 = 1.0$ (GeV/c) 2 . The fraction of events analyzed (0.8%) was essentially identical in both the data runs and calibration runs. In the data runs we obtained a total of about 7300 ($B_L + B_R$) events at $P_{\perp}^2 = 0.6$, 9100 at $P_{\perp}^2 = 0.8$, and about 12 000 at $P_{\perp}^2 = 1.0$ (GeV/c) 2 . These gave a statistical error of about 4% in each recoil polarization.

The two-spin cross sections and their associated Wolfenstein parameters A and C_{nn} were obtained from the data as before.^{1,3} However, in this high-statistics experiment we averaged out systematic errors such as beam drift by flipping the beam polarization on alternate pulses. This decreased our errors to about $\pm \frac{1}{3}\%$. Values of A and C_{nn} at each P_{\perp}^2 are given in Table I and Fig. 2 and are in good agreement with earlier measurements.^{2,3,5}

Using the measured recoil polarization, P_R , and the beam and target polarizations, P_B and P_T , we obtain the eight normalized three-spin cross-section ratios

$$\sigma_{ij \rightarrow oi} = \frac{d\sigma}{dt}(ij \rightarrow oi) / \left\langle \frac{d\sigma}{dt} \right\rangle. \quad (4)$$

Our notation is σ (beam, target \rightarrow scattered, recoil) and 0 denotes unmeasured, while i , j , and l specify the transversity spin states \uparrow or \downarrow .

$\langle d\sigma/dt \rangle$ is the differential cross section for an unpolarized beam and target.⁶ We now consider two additional Wolfenstein parameters,⁷

$$4D_{nn} = \sum_{ij} (\sigma_{ij \rightarrow oj} - \sigma_{ij \rightarrow oi}), \quad (5)$$

$$4K_{nn} = \sum_{ij} (\sigma_{ij \rightarrow oi} - \sigma_{ij \rightarrow oi}).$$

The parameter D_{nn} is the correlation between the recoil polarization P_R and the target polarization P_T and equals unity when the spin-flip cross section is zero. Similarly K_{nn} is the correlation between P_R and the beam polarization P_B and measures the spin transfer. These parameters are given in Table I and Fig. 2. Notice that D_{nn} may

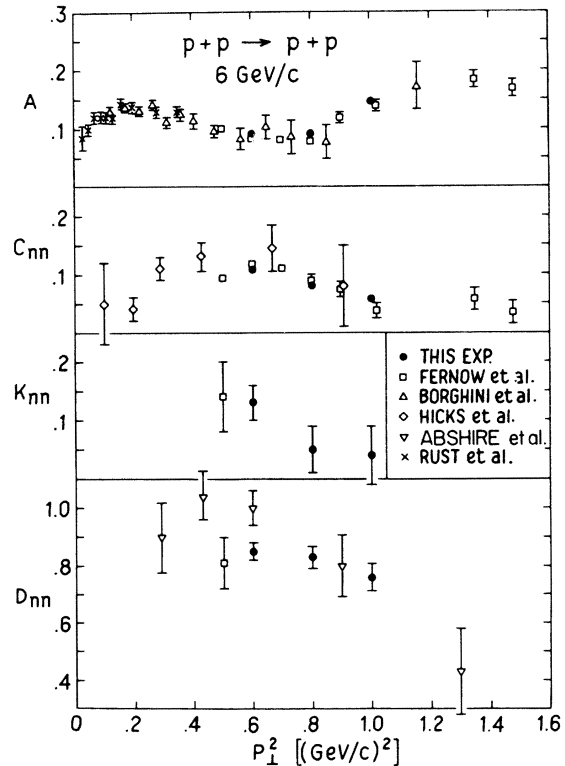


FIG. 2. Wolfenstein parameters for p - p elastic scattering at 6 GeV/c are plotted against P_{\perp}^2 . For some of the other experiments the bin sizes have been increased at large P_{\perp}^2 to improve the statistics.

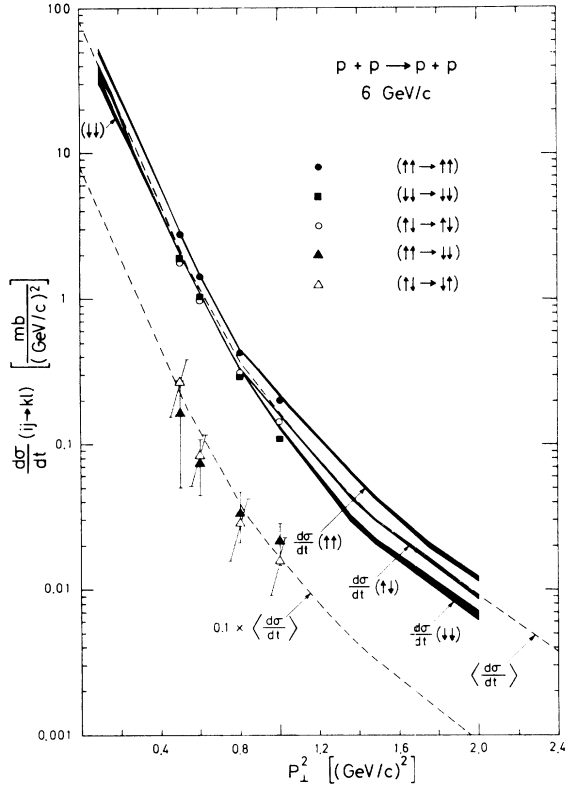


FIG. 3. Plot of the pure four-spin cross sections $d\sigma/dt(ij \rightarrow kl)$ for p - p elastic scattering at 6 GeV/c against P_{\perp}^2 . We also plotted the pure initial-two-spin cross sections $d\sigma/dt(ij)$ as bands with widths corresponding to the errors (see Ref. 3). Also shown as dashed lines are the spin-average cross section $\langle d\sigma/dt \rangle$ and 10% of $\langle d\sigma/dt \rangle$ for comparison with double-flip cross sections. Notice that $P_{\perp}^2 = 2.40$ (GeV/c) 2 corresponds to 90° cm at 6 GeV/c.

be moving further from 1 at large P_{\perp}^2 while K_{nn} may be moving toward 0. Our values of D_{nn} are smaller than those of Abshire *et al.*⁸ at the lower P_{\perp}^2 .

Each of the pure three-spin cross sections $\sigma_{ij \rightarrow 0l}$ is the sum of two pure four-spin cross sections

$$\sigma_{ij \rightarrow 0l} = \sigma_{ij \rightarrow \uparrow l} + \sigma_{ij \rightarrow \downarrow l} . \quad (6)$$

For identical particles rotational invariance requires that

$$\sigma_{\uparrow\uparrow \rightarrow \uparrow\uparrow} = \sigma_{\uparrow\uparrow \rightarrow \downarrow\downarrow} , \quad (7)$$

$$\sigma_{\uparrow\downarrow \rightarrow \uparrow\downarrow} = \sigma_{\uparrow\downarrow \rightarrow \uparrow\uparrow} .$$

In addition, parity invariance requires⁹ that all eight single-flip transversity cross sections equal zero. Using (7) we can test for a possible parity violation by forming the experimental quantity

$$\epsilon_P = \sigma_{\uparrow\uparrow \rightarrow 0\downarrow} - \sigma_{\uparrow\downarrow \rightarrow 0\uparrow} = \sigma_{\uparrow\uparrow \rightarrow \downarrow\downarrow} - \sigma_{\uparrow\downarrow \rightarrow \uparrow\uparrow} . \quad (8)$$

Parity conservation requires ϵ_P to be zero. Our results for ϵ_P are: 0.07 ± 0.05 at $P_{\perp}^2 = 0.6$, 0.08 ± 0.06 at $P_{\perp}^2 = 0.8$, and 0.00 ± 0.08 at $P_{\perp}^2 = 1.0$, showing no evidence for a parity violation at any P_{\perp}^2 .

Time-reversal invariance imposes another relation among the pure four-spin transversity cross sections

$$\sigma_{\uparrow\uparrow \rightarrow \downarrow\downarrow} = \sigma_{\downarrow\downarrow \rightarrow \uparrow\uparrow} . \quad (9)$$

Since there is no evidence of a P violation we can form a quantity ϵ_T ,

$$\epsilon_T = \sigma_{\uparrow\uparrow \rightarrow 0\downarrow} - \sigma_{\uparrow\downarrow \rightarrow 0\uparrow} = \sigma_{\uparrow\uparrow \rightarrow \downarrow\downarrow} - \sigma_{\uparrow\downarrow \rightarrow \uparrow\uparrow} , \quad (10)$$

which tests T invariance. Our results for ϵ_T are: -0.01 ± 0.05 at $P_{\perp}^2 = 0.6$, 0.02 ± 0.06 at $P_{\perp}^2 = 0.8$ and 0.11 ± 0.08 at $P_{\perp}^2 = 1.0$, showing no evidence for a T violation.

In Fig. 3 we have plotted the five $d\sigma/dt(ij \rightarrow kl)$ against P_{\perp}^2 . The $\langle d\sigma/dt \rangle$ we used⁶ is shown as a dashed line. We have also plotted the three initial-two-spin cross sections as bands whose widths correspond to the error at each P_{\perp}^2 . These errors are much smaller than those of the four-spin cross sections because the recoil-polarization error does not contribute. For $P_{\perp}^2 \geq 0.5$ (GeV/c) 2 these $d\sigma/dt(ij)$ were obtained from Table I and our earlier publication,³ while for $P_{\perp}^2 \leq 0.4$ we combined the C_m measurements of Hicks *et al.*² with the A measurements of Borghini *et al.*⁵

The most important feature of Fig. 3 is that the different spin states have quite unequal cross sections. The parallel-up cross sections $d\sigma/dt(\uparrow\uparrow \rightarrow \uparrow\uparrow)$ and $d\sigma/dt(\uparrow\uparrow)$ are sometimes twice as large as the parallel-down $d\sigma/dt(\downarrow\downarrow \rightarrow \downarrow\downarrow)$ and $d\sigma/dt(\downarrow\downarrow)$. The double-flip cross sections, $d\sigma/dt(\uparrow\uparrow \rightarrow \downarrow\downarrow)$ and $d\sigma/dt(\uparrow\downarrow \rightarrow \uparrow\uparrow)$, are typically 10 times smaller than the nonflip. These large differences imply that spin must be considered in any serious model for strong interactions.¹⁰

Another very striking feature is the clear change in the spin dependence near $P_{\perp}^2 = 0.8$ (GeV/c) 2 , where $\langle d\sigma/dt \rangle$ has a break. In the "diffraction peak" region below the break the $d\sigma/dt(ij \rightarrow kl)$ are all parallel to each other and $d\sigma/dt(\uparrow\uparrow \rightarrow \uparrow\uparrow)$ is about 50% larger than both $d\sigma/dt(\uparrow\downarrow \rightarrow \uparrow\uparrow)$ and $d\sigma/dt(\downarrow\downarrow \rightarrow \downarrow\downarrow)$. The cross sections have much more spin dependence in the region after the break where the $d\sigma/dt(ij)$ are again parallel but now with a slope of $\sim e^{-3.5P_{\perp}^2}$. Here $d\sigma/dt(\uparrow\uparrow \rightarrow \uparrow\uparrow)$ is 100% larger than $d\sigma/dt(\downarrow\downarrow \rightarrow \downarrow\downarrow)$, while $d\sigma/dt(\uparrow\downarrow \rightarrow \uparrow\uparrow)$ is about halfway between.

There is some indication that the double-flip cross sections, especially $d\sigma/dt(\uparrow\uparrow \rightarrow \downarrow\downarrow)$, may be relatively larger after the break. This can also be seen by studying D_{nn} in Fig. 2. This ef-

fect is a few standard deviations and thus is not certain, but it is an interesting possibility. It would be very significant if the double-flip cross section became dominant at very large P_{\perp}^2 .

The break in $d\sigma/dt$ corresponds to the transition from the forward diffraction peak to the large- P_{\perp}^2 region. The large spin dependence in this second region may give important information about the nature of large- P_{\perp}^2 elastic scattering. We plan to study this further by extending these measure-

ments to larger P_{\perp}^2 .

We are very grateful to the ZGS staff for the improved operation of the polarized beam. We thank Dr. S. W. Gray and Dr. E. F. Parker for their help in the early stages of the experiment and J. A. Bywater, W. Dragoset, H. E. Haber, J. G. Toney, and A. L. Weil for their help in running. A.D.K. thanks the Niels Bohr Institute for their hospitality while this paper was being written.

*Work supported by the U.S. Energy Research and Development Administration.

†Present address: Max Planck Institute für Physik, Munich, Germany.

‡Presently on leave at Niels Bohr Institute, Copenhagen, Denmark.

§Present address: NP Division, CERN, Geneva, Switzerland.

||Present address: Rice University, Houston, Texas.

¹J. O'Fallon *et al.*, Phys. Rev. Lett. 32, 77 (1974); H. E. Miettinen, thesis, University of Michigan, 1975 (unpublished).

²G. Hicks *et al.*, Phys. Rev. D 12, 2594 (1975).

³R. Fernow *et al.*, Phys. Lett. 52B, 243 (1974).

⁴L. G. Ratner *et al.*, unpublished work.

⁵M. Borghini *et al.*, Phys. Lett. 31B, 405 (1971); D. Rust *et al.*, *ibid.* 58B, 114 (1975).

⁶I. Ambats *et al.*, Phys. Rev. D 9, 1179 (1974).

⁷G. Schumacher and H. Bethe, Phys. Rev. 121, 1534 (1961).

⁸G. Abshire *et al.*, Phys. Rev. Lett. 32, 1261 (1974); Phys. Rev. D 12, 3393 (1975).

⁹A. Bohr, Nucl. Phys. 10, 486 (1959).

¹⁰C. Bourrely, J. Soffer, and D. Wray, Nucl. Phys. B77, 386 (1974); Phys. Lett. 43B, 514 (1973); Nucl. Phys. B85, 32 (1975); B91, 33 (1975); A. W. Hendry and G. W. Abshire, Phys. Rev. D 10, 3362 (1974); E. Gotsman and U. Maor, Nucl. Phys. B96, 167 (1975); G. L. Kane and U. P. Sukhatme, Nucl. Phys. B78, 110 (1974); F. Halzen and G. H. Thomas, Phys. Rev. D 10, 344 (1974); Proceedings of the 1974 Argonne Summer Study on High Energy Physics with Polarized Beams, edited by J. B. Roberts [Argonne National Laboratory Report No. ANL/HEP 75-02; 1974 (unpublished)].